Supporting Information For:

XeNA: An automated 'open-source' ^{129}Xe hyperpolarizer for clinical use

Panayiotis Nikolaou[a,b], Aaron M. Coffey[a,i], Laura L. Walkup[b†], Brogan M. Gust[b], Nicholas Whiting[c*], Hayley Newton[c], Iga Muradyan[e], Mikayel Dabaghyan[e], Kaili Ranta[d], Gregory D. Moroz[f], Matthew S. Rosen[g,h], Samuel Patz[e], Michael J. Barlow[c], Eduard Y. Chekmenev[a,i,j], and Boyd M. Goodson[b]

[a]Department of Radiology, Vanderbilt University Institute of Imaging Science (VUIIS), Nashville, TN, 37232, United States; [b]Department of Chemistry & Biochemistry, Southern Illinois University, Carbondale, IL; [c]Sir Peter Mansfield Magnetic Resonance Centre, University of Nottingham, Nottingham, NG7 2RD, UK; [d]Department of Physics, Southern Illinois University, Carbondale, IL; [e]Department of Radiology, Brigham & Women's Hospital and Harvard Medical School, Boston, MA; [f]Graduate School Central Research Shop, Southern Illinois University, Carbondale, IL; [g]MGH/A.A. Martinos Center for Biomedical Imaging, Boston MA; [h]Department of Physics, Harvard University, Cambridge MA ; [i]Department of Biomedical Engineering, Vanderbilt University, Nashville, Tennessee, 37235, United States; [j]Department of Biochemistry, Vanderbilt University, Nashville, Tennessee, 37205, United States

[†]*Present address: Cincinnati Children's Hospital Medical Center, Cincinnati, OH*

**Present address: MD Anderson Cancer Center, Houston, TX*

Corresponding Authors: Boyd M. Goodson, Department of Chemistry & Biochemistry, Southern Illinois University, Carbondale, IL. Phone: 618-453-6427; Fax: 618-453-6408;

E-mail: bgoodson@chem.siu.edu

And

Panayiotis (Peter) Nikolaou, Department of Radiology, Vanderbilt University Institute of Imaging Science, Nashville, TN. Phone: 618-203-6912

E-mail: peter.nikolaou@vanderbilt.edu

Keywords: hyperpolarization, MRI, laser-polarized xenon, optical pumping, lung imaging

Overview:

This supporting information provides additional pertinent details about the polarizer's construction, functionality, and operational procedures to facilitate reproduction or adaptation of the xenon hyperpolarizer device. Section (a) contains details about the lower frame and organization of equipment used to operate the various components of the polarizer (including much of the gas manifold); Section (b) concerns the upper frame; Section (c) provides details about the laser and optical assembly, including a detailed parts list of the components used; Section (d) discusses the optical assemblies behind the oven for beam retro-reflection and near-IR detection; Section (e) provides dimensions of the OP-oven along with 3D-CAD drawings, as well as additional details about the OP-cells; Section (f) provides information regarding the GUI and its operation; Section (g) describes *in situ* monitoring of $\langle P_{Rb} \rangle$; Section (h) provides additional details concerning low-field NMR results used to observe Xe polarization dynamics and calibrate P_{Xe}; Section (i) describes the OP-cell cool-down procedure we have implemented to help better maintain high P_{Xe} values through the HP ^{129}Xe-transfer process; and Section (j) provides additional information about our use of Tedlar bags to transport and deliver the HP ^{129}Xe to the high-field MRI scanner. Although most of the text below provides details about what is actually in the XeNA polarizer, where relevant, alternative solutions are provided. Along with the Main Document, the reader is directed to Ref. [S1] for additional information about HP ^{129}Xe results and analysis.

a) Lower Frame: The lower chassis of the polarizer is comprised of two 19" rack-mountable cabinets; while for XeNA the empty cabinets of a surplus Varian Inova console were used, any pair of cabinets of sufficient ruggedness and size would be appropriate (e.g., www.rackmountsolutions.net P/N KH 3100-3-001-22). The left rack-mountable cabinet (**Fig. S1a)** houses the gas-handling equipment. These components first consist of: (1) An Edwards Rotary Vane (RV) 5 mechanical roughing vacuum pump, which is used to evacuate the gas-handling lines to a level (~10^{-3} Torr) that enables safe operation of: (2) an Edwards Turbo Pump Station (TS75W), which allows the manifold to reach down to the ~10^{-5} Torr regime (to reducing the partial pressure of O_2 in the gas-handling and thereby prevent depolarization of HP ^{129}Xe gas or degradation/oxidation of the Rb alkali metal in the OP-cell). Both these vacuum systems are mounted to a supporting base of ¼" aluminum plate. Most of the gas manifold (3) is also mounted in this portion of the chassis. The gas-loading ('upstream') section of the manifold includes solenoid valves (McMaster-Carr P/N 5077T123) and ¼" stainless steel metal tubing. These components are depolarizing to HP gases, but the upstream region of the system is free from exposure to HP ^{129}Xe gas. The valves are each actuated by a 24 V DC supply directed through solid-state relays that are driven by the Arduino Microcontroller. Typical of these valves is their tendency to run hot when their solenoid is energized ('open') for extended periods of time during polarizer operation. The valve temperatures are mitigated with a small heat sink (P/N 8822T13, McMaster Carr) attached to the housing of each of the solenoid valves via thermal transfer tape and held into position

with epoxy. The valves themselves are bolted to an aluminum plate and connected to lines via ¼" Swagelok fittings, and laid out as shown in main **Fig. 1a**. All Swagelok components and associated tubing were purchased from regional Swagelok suppliers (e.g. St. Louis Valve and Fitting, Union Tees P/N SS-400-3, Union Straights PN SS-400-6, Union Crosses P/N SS-400-4, and Union Elbows P/N SS-400-9). *Additional notes*: although the above components are cost-effective (and do not take up much space), chasing down leaks and replacing components is challenging in a Swagelok-based gas handling system. Thus, despite the increased costs and bulk, the authors recommended that VCR-style fittings be used throughout the 'up-stream' (non-HP-^{129}Xe-contacting) portion of the manifold, along with a different model of valve (e.g., Parker P/N 099-0167-900).

The HP ^{129}Xe gas-transfer section (4—*Inset* **Fig. S1a**) of the manifold ('downstream' of the OP-cell) is located inside the laser enclosure and consists of pneumatically actuated, Teflon-sealed valves (Teqcom P/N M222CPFS-T) and Teflon (1/4" PTFE) tubing. These valves and materials are chosen to reduce depolarization of HP ^{129}Xe gas that might otherwise occur through (i) exposure to resonant magnetic fields produced by actuating solenoids that could drive spin flops; (ii) physical contact with paramagnetic sites; and/or (iii) passing through magnetic-field zero-crossings. Moreover, these lines are kept as short as possible to ensure better vacuum quality. The transfer line is also equipped with an Entegris Wafergard GT-Plus gas filter (5—*Inset* **Fig. S1a**), placed in-series up-stream of the gas line leading to the sample / Tedlar bag, to prevent any residual vaporized Rb (or any other particulate matter) from being transferred to the sample or HP ^{129}Xe-transport container of interest. The lower frame is air-cooled with a rack-mounted fan bank at the rear of the left cabinet. Although the prototype was built with previously-existing fan equipment, a good solution is: P/N UQFP-4 from Rackmount Solutions.

The right rack-mountable cabinet (**Fig. S1b**) houses all major electronics and instrumentation used to power and control the different components of the polarizer. These components include: (1) a Kenwood PSU (power supply unit) (P/N PDS60/12) used to generate the current for the four electromagnetic coils (which provide the magnetic field for SEOP and low-field NMR detection); (2) the Omega i-series temperature controller responsible for regulating the optical pumping oven temperature during the SEOP process (via the heatpipes); (3) Teledyne Hastings HPM 2002 fine vacuum gauge; (4) PSU for the 200 W LDA (Xantrex, model XFR 20-60); (5) utility drawer (for laser goggles, software, hardware parts storage, etc. (P/N UD3, www.RackmountSolutions.net)); (6) Sliding shelf for computer laptop support (P/N SS1920-V, www.RackmountSolutions.net); (7) the Magritek Kea2 NMR low-frequency spectrometer used for *in-situ* monitoring of P_{Xe} during and after SEOP; (8) Micro-controller Automation box responsible for sensor monitoring and automation procedures (see also Fig. 4 of the Main Document); and (9) 800 W K-O Concepts water chiller used to cool the 200 W LDA and provide fine control of the LDA temperature to tune the LDA's output frequency. All instrumentation in the lower frame is powered through two large rack-mounted power strips, which in turn are plugged into wall

outlets (110 VAC, 20 A each) to power the hyperpolarizer. The dimensions of the lower frame can be found in **Fig. S2**.

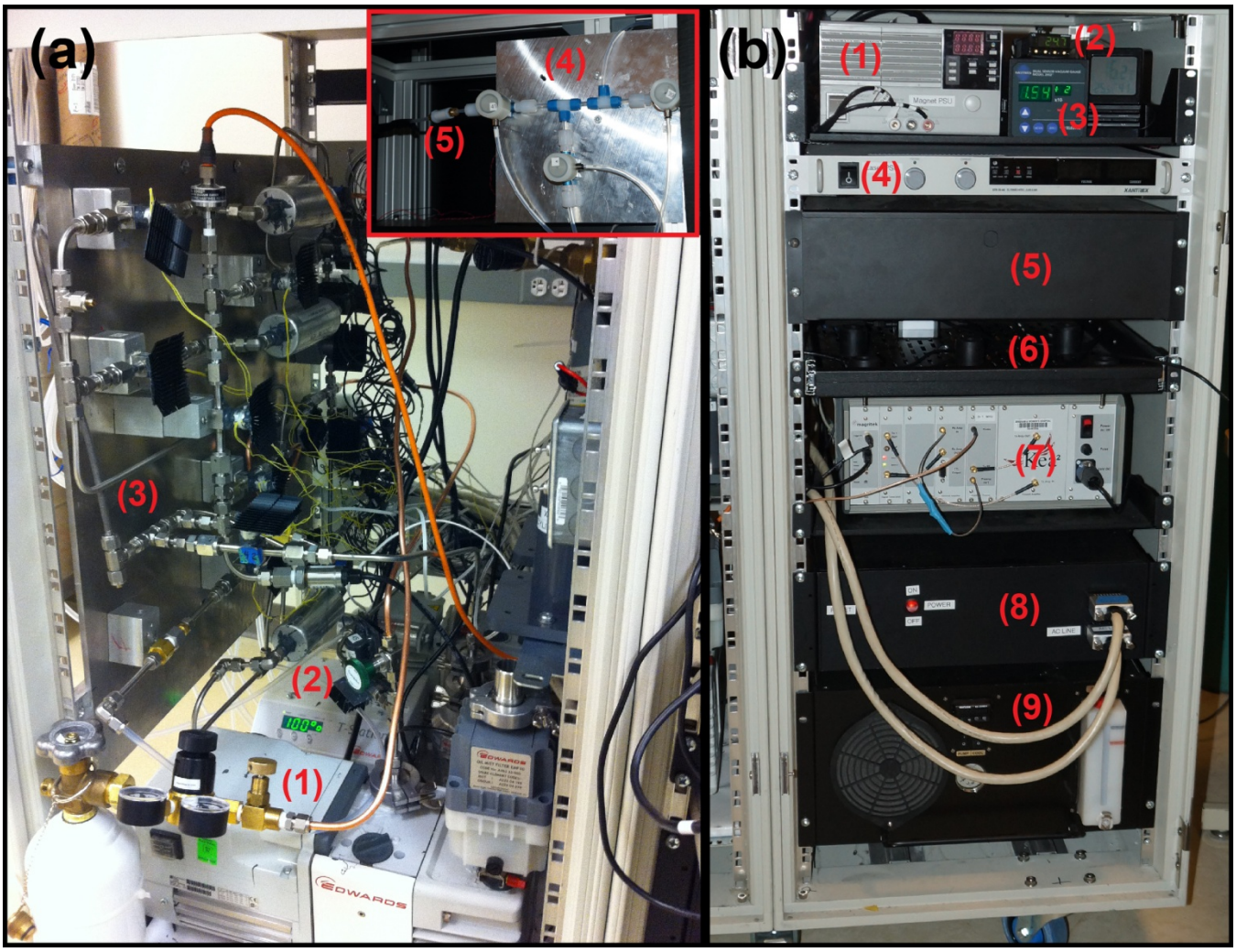

Figure S1. (*A*) Left cabinet space of rack-mountable chassis containing: (*1*) mechanical vacuum pump (Edwards RV5); (*2*) Edwards Turbo Pump Station model #TS75W; (*3*) Gas handling manifold—gas-loading ('upstream') section; (*4*) gas transfer ('downstream') section; (*5*) gas filter (Entegris Wafergard GT-Plus). One 'oversized' gas cylinder (Xe) can be seen at the lower left; the other gas cylinders are hidden from view along the inside wall of the cabinet. **(*B*)** (*1*) Kenwood electromagnet power supply, (*2*) Omega i-series temperature controller, (*3*) Teledyne Hastings HPM 2002 fine vacuum gauge, (*4*) LDA PSU, *Inset:* (*5*) utility drawer, (*6*) Sliding shelf for computer laptop, (*7*) low-field NMR spectrometer (Magritek, Kea2), (*8*) Micro-controller Automation box, (*9*) 800 W water chiller (K-O Concepts, model LCR-8)

b) Upper Frame: The upper frame (**Fig. S2**) extends beyond the horizontal length of the lower frame due to the space requirements of the laser and the optical path/assembly. For example, it was necessary to leave sufficient room between the optics assembly and the front face of the oven to allow convenient access for a large fan-cooled laser power meter head (to monitor the lasers output during the testing stages). Not shown in the figure below is the laser enclosure: On the four corners of the frame, Vertical T-slotted rails were placed on the four corners of the frame possessing sufficient height to ensure that the roof of the enclosure would clear the top of the electromagnetic coils (but still short enough to ensure vertical clearance for the polarizer to fit through ~7' doorways); these vertical rails are connected with 672 and 1721 mm horizontal rails to form the skeleton of the rectangular enclosure. T-

slotted rails have a cross-sectional profile of 45 x 45 mm, **Fig. S2a**. To this frame we attached the appropriate-sized Alumalite laser enclosure panels (corrugated plastic core with 0.013" thick matte black painted aluminum skins on both sides; Minitec Framing). Also not shown in the figure below is a door that opens upwards, constructed from T-slotted rails (seen in **Fig. 1b**) and an Alumalite panel. *Note*: the Minitec Framing special "power-lock" bolts (http://youtu.be/IJSgDXNBkRc) that lock the T-slotted rails in place are slightly magnetic; however, these pieces were sufficiently far from the cell and the NMR detection coil that no detrimental effects were detected in the NMR spectra.

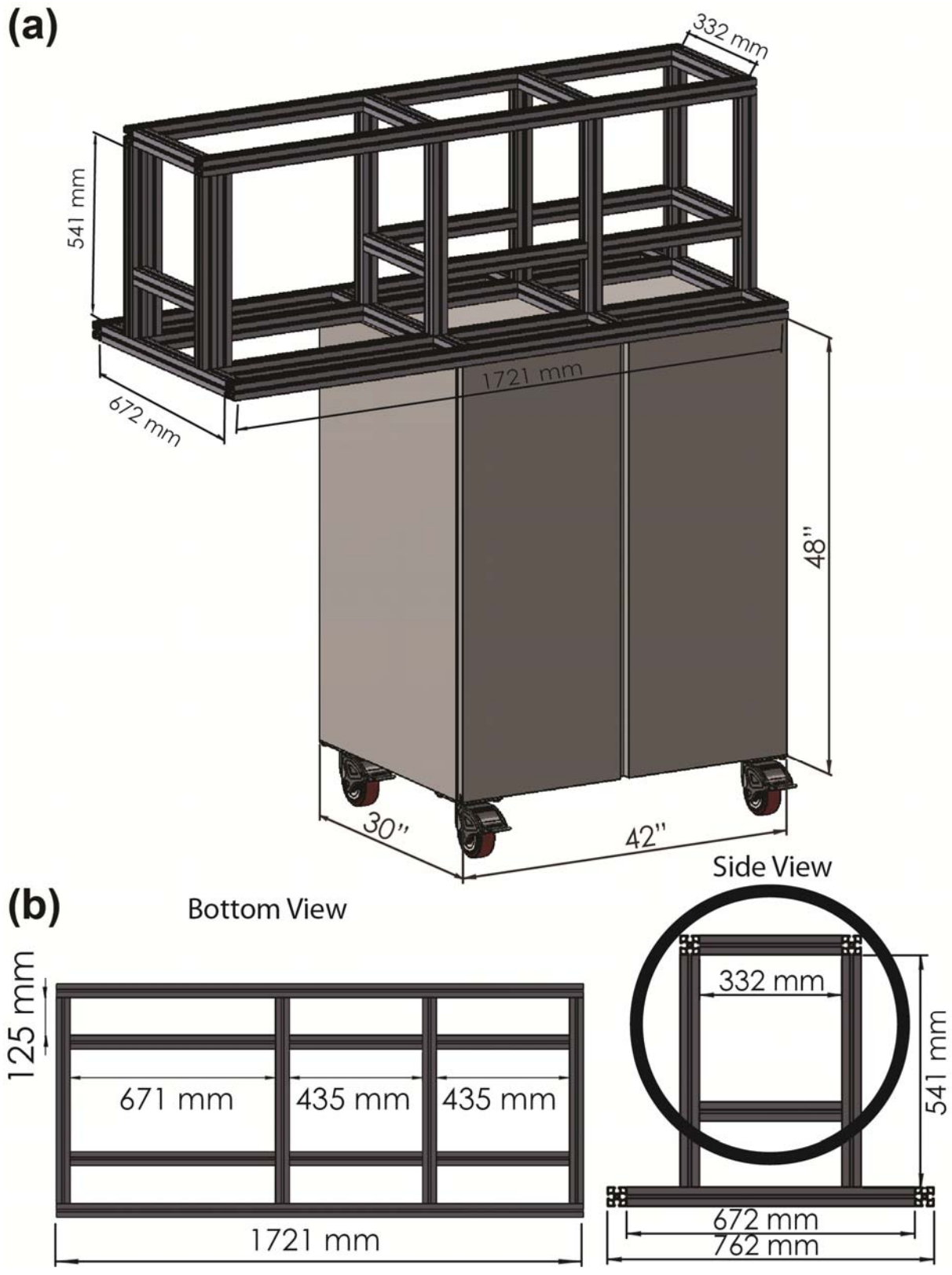

Figure S2. (*a*) CAD drawing showing the dimensions of the lower frame (rack-mounted cabinets) with the upper frame attached to it. (*b*) CAD drawings of the upper frame with dimensions.

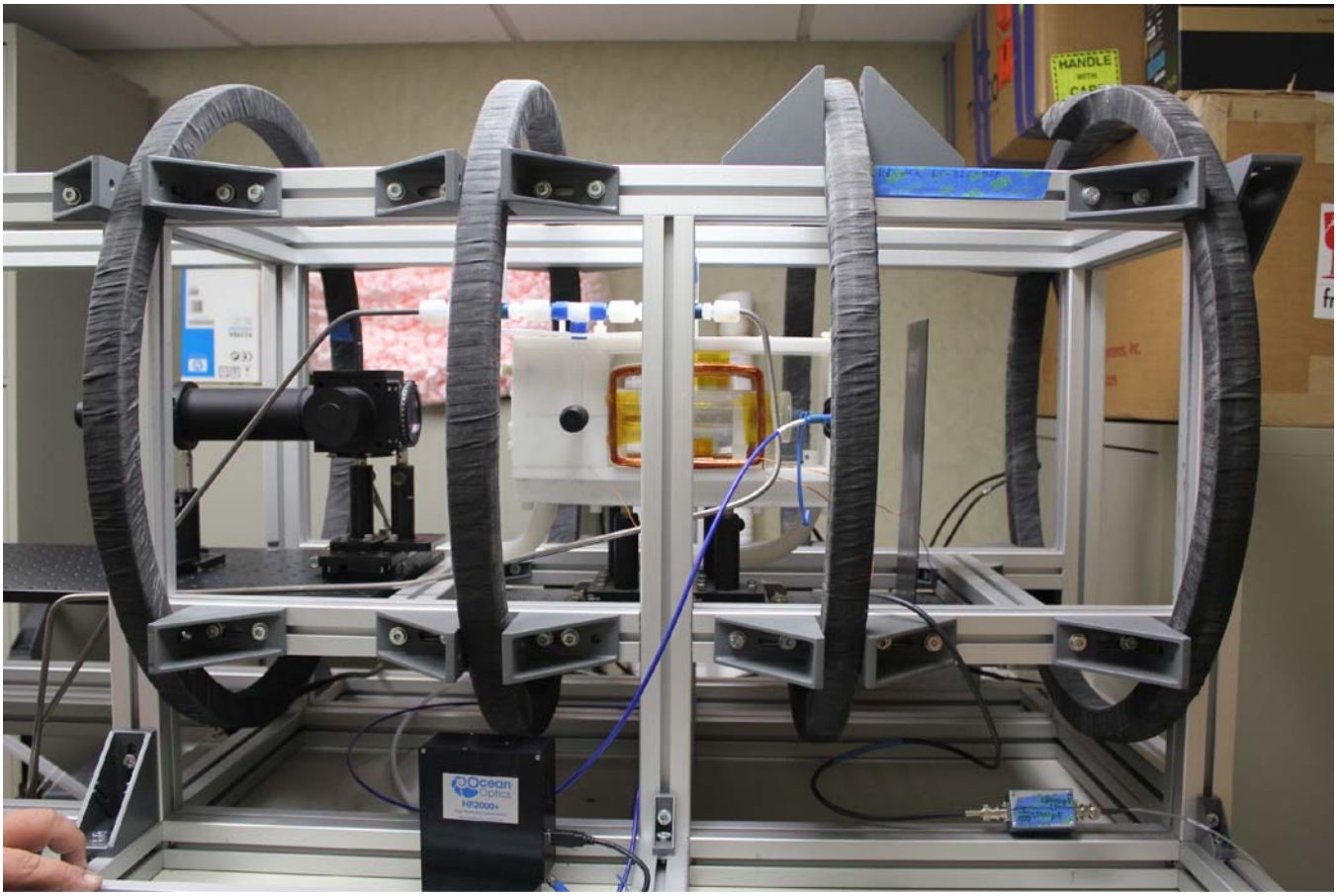

Figure S3. Corresponding photo of the right-most part of the upper frame, at a relatively early stage of polarizer construction—showing the positions of the electromagnetic coils; nominal center-to-center spacing is approximately 12 in, not including slight adjustments from shimming.

c) Optical Path/Assembly: A complete parts list for the optical assembly can be found below in **Table S1**. The optical assembly begins with (1) the 200 W QPC laser and its short solid fiber with an 800 μm bore. Next, (2) a (*x,y*) translating lens mount is used to align the output of the LDA with a 4.03 mm focal length aspheric lens (Thorlabs P/N C340TME-B). The lens slows the natural expansion of the LDA output from the fiber, allowing it to expand to just under 2" diameter within the lens tube (3), where the beam is colimated using a 2" diameter N-BK7, 75 mm focal length plano-convex lens (Thorlabs P/N LA1145-B). (5) The 2" polarizing beam-splitter (PBS) cube is contained in a 60 mm housing, which had to be machined to allow the PBS cube to slide into place correctly. The *s*-polarized beam component is reflected 90° to the right and discarded into a beam block (4); the main (*p*-polarized) beam is transmitted forward into a quarter-wave (λ/4) plate (6), which renders the beam circularly-polarized. Not seen in the figure below is an additional beam block on the opposite side of the PBS housing which absorbs the beam returning from the oven, reflected 90° into it by the PBS. Due the high power of the laser, these beam blocks tend to get extremely hot, so to aid with cooling we installed a fan (7) directly beneath each beam block to direct air over their cooling fins.

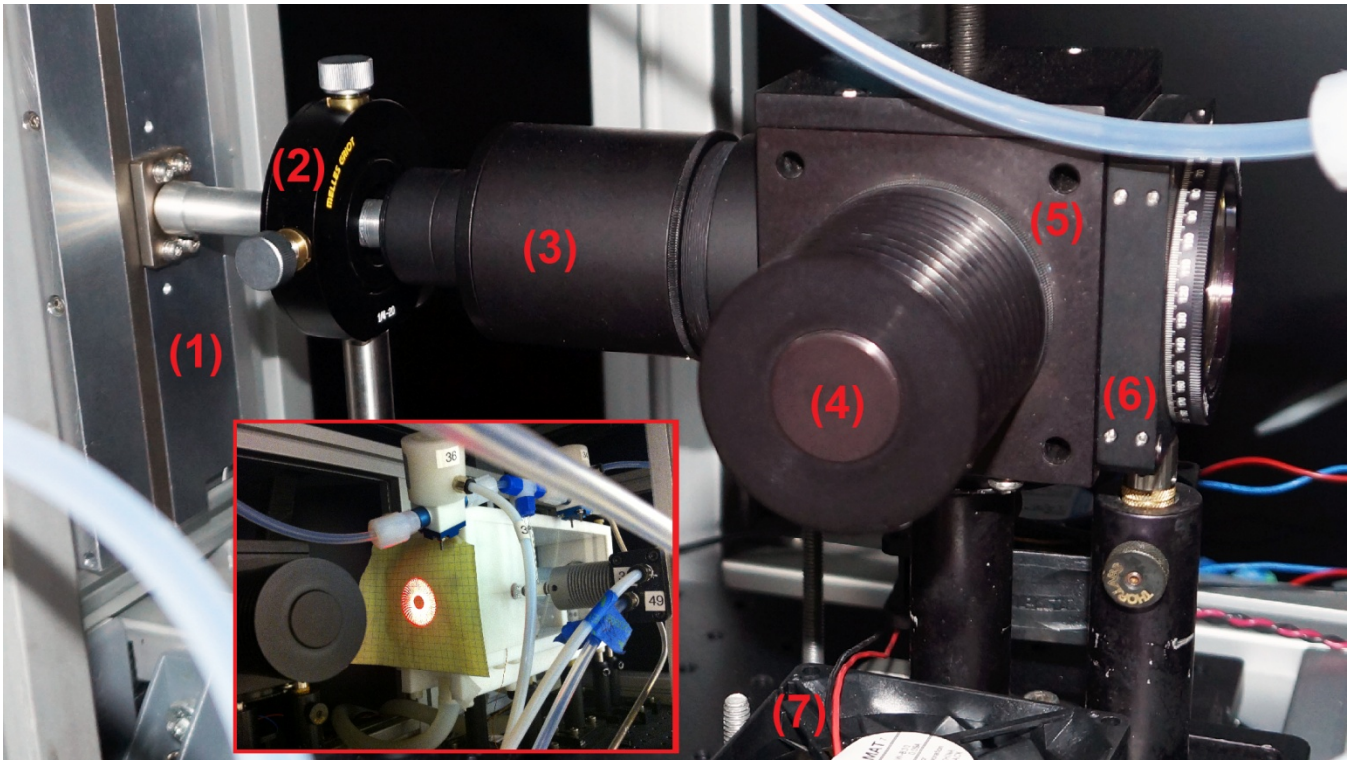

Figure S4. Components of the optical assembly. (1) LDA with short 800 μm bore fiber; (2) Translational lens mount; (3) lens tube; (4) beam block; (5) 60-mm housing for the PBS cube; (6) quarter-wave (λ/4) plate location; (7) fan used to cool a beam block. ***Inset*:** Aiming beam from the laser, passed through the optical assembly and expanded to 2" diameter, used for aligning the laser with the OP-cell.

The 200 W LDA (QPC Lasers, P/N 6507-0001 Brightlock Ultra-500) utilizes "on-chip" volume holographic grating (VHG) technology wherein the gratings are written at the wafer level during Metal-Organic Chemical Vapor Deposition (MOCVD); such LDAs possess output with an order-of-magnitude narrower spectral output (FWHM~0.2-0.3 nm) compared to conventional LDAs (~2-3 nm) (**Fig. S5a**). The improved line shape and laser spectral output results in increased resonant photon flux for Rb absorption at the D_1 line (nominally at 794.76 nm). The LDA housing is mounted to a water-cooled plate; this water-cooled LDA design allows the spectral output to be tuned over a range of ~1 nm—or alternatively allows the laser centroid wavelength to be held at the same value—by simply adjusting the changing the laser's diode temperature appropriately when varying the laser driving current (**Fig. S5b**). Variation of the laser diode temperature results in only fine changes in spectral output, whereas variation of laser driving current results in more coarse adjustments. *Note*: Because very good results were achieved with this laser and optical assembly in XeNA polarizer, more recently we have worked with QPC to design an integrated solution based on this proven design. In this new design (Nikolaou, *et al.* manuscript in preparation) all of the polarizing optics are mounted directly to the laser chassis, greatly simplifying operation and beam alignment (QPC, P/N 6507-Z002). Finally, we generally chose optics that would *also* allow us to use the same optical path to allow SEOP with Cs at its D1 wavelength of 894.3 nm.

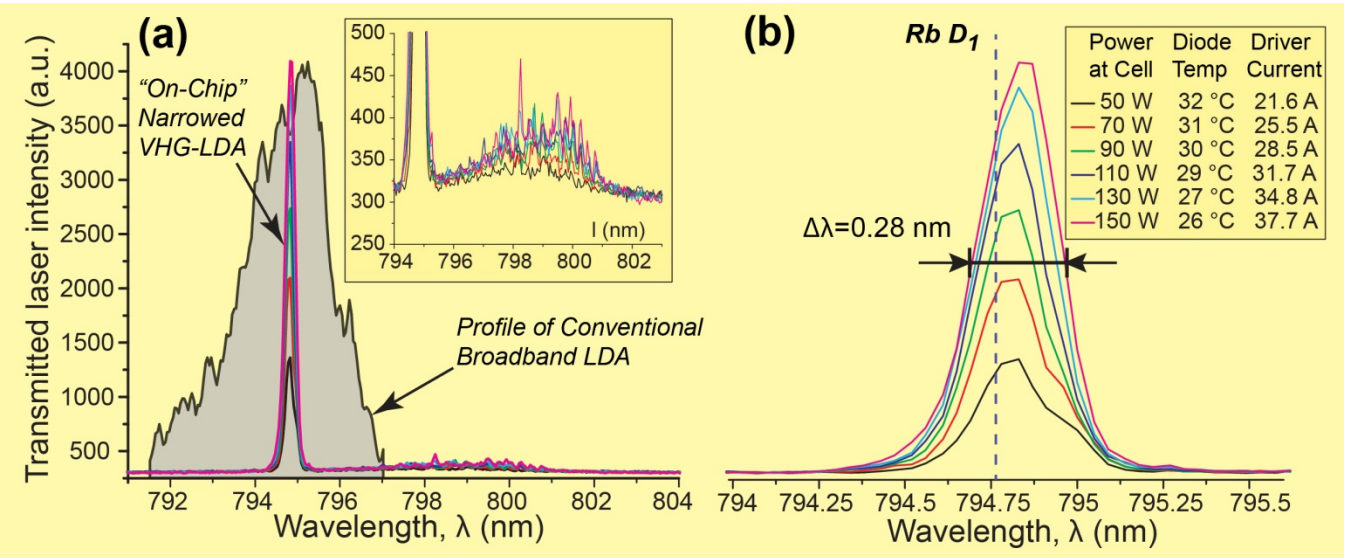

Figure S5. Spectral profiles of output from a 200 W near-IR VHG-LDA from QPC. (a) Comparison of VHG-narrowed spectral output compared to that of a conventional LDA (normalized to the same vertical scale). The more favorable line shape of the VHG-narrowed LDA results in greater Rb absorption efficiency. The *inset* shows a close-up of the (generally weak) unlocked portion of the LDA output typically found at longer wavelengths. (b) Close-up of the main region of the spectra shown in (a), with the position of the nominal Rb D_1 line demarked with a vertical dotted line. Nominal FWHM: 0.28 nm. The inset contains a table of the LDA temperature / LDA PSU driver current combinations that provide the displayed output fixed at the same centroid wavelength, along with the corresponding output powers.

Table S1A: Parts list for the optical assembly; parts from Thorlabs.com unless otherwise stated	
LM05XY	Translating Lens Mount for Ø1/2" Optics
LB3C	Rotatable Cage Cube Platform for LC6W
LA1145-B	N-BK7 Plano-Convex Lens, Ø2", f = 75.0 mm, ARC: 650-1050 nm
SM2T2	SM2 (Ø2.035"-40) Coupler, External Threads
LB4C	Rotatable Kinematic Cage Cube Platform for LC6W
LB6C	60 mm Cube Clamp
LCRM2	60 mm Cage Rotation Mount for Ø2" Optics
SM2CP2	SM2 Series End Cap, External Thread
ER1	Cage Assembly Rod, 1" Long, Ø6 mm, Qty. 1
LC6W	60 mm Cage System Cube with Ø6 mm Clearance Holes
SM2T2	SM2 (Ø2.035"-40) Coupler, External Threads
SM2E60	6" Extension Tube for SM2 Lens Tube, One Retaining Ring Included
SM2L20	SM2 Lens Tube, 2" Thread Depth, One Retaining Ring Included
SM2L05	SM2 Lens Tube, 0.5" Thread Depth, One Retaining Ring Included
SM1A2	Adapter with External SM1 Threads and Internal SM2 Threads
SM1T1	SM1 (Ø1.035"-40) Coupler, Internal Threads
SM1SMA	SM1 (1.035"-40) to SMA Fiber Connector Adapter Plate
LA1050-B	N-BK7 Plano-Convex Lens, Ø2", f = 100.0 mm, ARC: 650-1050 nm
LA1401-B	N-BK7 Plano-Convex Lens, Ø2", f = 60.0 mm, ARC: 650-1050 nm
C340TME-B	f = 4.03 mm, NA = 0.62, Mounted Aspheric Lens, AR: 600-1050 nm
HSLT1	Passive Heat Sink SM1 Lens Tube
SM1PL	SM1 Plug
R2	Slip-On Post Collar For Ø1/2" Posts
TRT2	Translating Ø1/2" Optical Post: 2" to 2 1/4"
SPW604	Spanner Wrench with Clear Aperture for SM2 Retaining Rings
ER05	Cage Assembly Rod, 1/2" Long, Ø6 mm
SM2V10	Ø2" SM2 Rotating Adjustable Focusing Element, 0.81”
PBSH-670-980-200	Polarizing Beam Splitting Cube, from **CVI-Melles Griot**
NQ-200-0839	Ø2" Quarter-Wave Plate, from **Meadowlark Optics**

Table S1B: Thorlabs.com parts list for Retro-Reflection	
SM1L05	SM1 Lens Tube, 0.5" Thread Depth, One Retaining Ring Included
SM1SMA	SMA Fiber Adapter Plate with External SM1 (1.035"-40) Thread
SM1RC	Ø1" (SM1) Series Slim Lens Tube Slip Ring, 8-32 Tapped Hole
SM1D12SZ	SM1-Threaded Zero Aperture Iris, Ø12 mm Max Aperture
BB3-E03	Ø3" Broadband Dielectric Mirror, 750-1100 nm
KS3	Ø3" Precision Kinematic Mirror Mount, 2 Adjusters
TR4	Ø1/2" x 4" Stainless Steel Optical Post, 8-32 Stud, 1/4"-20 Tapped Hole
PH4	Post Holder with Spring-Loaded Hex-Locking Thumbscrew, L = 4.00"
BA1	Mounting Base, 1" x 3" x 3/8"

d) Retro-Reflection and IR detection: The components used to make these items are listed in **Table S1B.** The retro-reflection mirror in its mount (1) reflects ~99% of the laser light back through the oven and the OP-Cell, and its angle of reflection can be finely adjusted using the mirror mounting stage in either the *x* or *y* axis (with the *z* axis being along the laser path). The ~1% of light that does pass through the mirror is used to monitor the laser's transmitted spectral profile, with particular interest concerning the light absorption by the Rb vapor, as recorded by a near-IR spectrometer (not shown here, but visible in a temporary location in Fig. S3). Instead of using a neutral density filter to reduce the amount of light picked up the IR spectrometer fiber-optic cable (3), an optical iris (2) was instead used, allowing the amount of light impinging on the fiber-optic cable to be varied by manually adjusting the aperture (depending on the laser power used) to prevent saturation of the IR spectrometer's response.

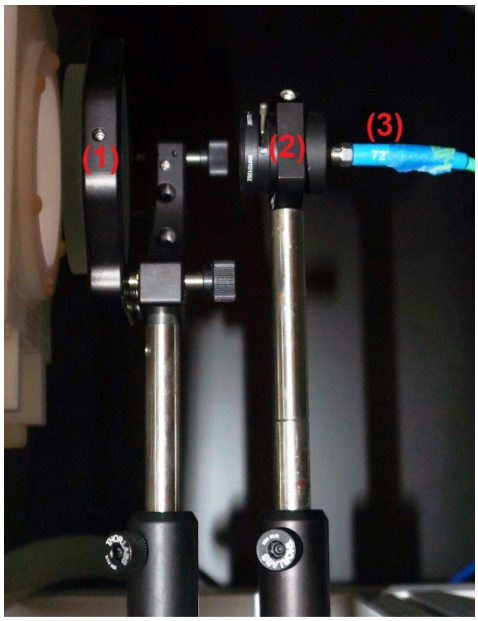

Figure S6. (1) Retro-reflection Mirror, (2) Adjustable Iris, (3) Fiber-Optic Cable leading to Near IR spectrometer.

e) Optical Pumping Oven and Cell: The main body of the oven, lens holders, lid, and OP-cell side stem holder were machined from Teflon sheets, and held together by a combination of Nylon and Teflon screws. The walls and lid of the oven are 0.5" thick while rails below the base were made 1" thick to provide greater structural integrity and support. Insets were grooved in the front and back to house 3" AR-coated optical windows and held in place using lens holders. The OP-cell's mounts feature a snug "snap into place" design to support the OP-cell, thus making the installation and removal of the cell effortless once the oven top has been removed. The OP-cell stem holder keeps the cell from sliding back and forth and helps align the Chemglass stopcock valve of the cell with the Helical-rotary actuator assembly. The sides of the oven use custom-cut Pyrex glass windows to serve as view ports into the oven, while still maintaining the oven's thermal integrity for heating and cooling. CAD drawings of the oven are shown in **Fig. S7a**, and additional photos at different stages of the XeNA-development process are shown in **Figs. S7b-e**. *Note*: The OP-oven may reach temperatures of up to ~120 ºC or hotter, depending on one's conditions (although we rarely operated the oven temperature above 80 ºC during SEOP). At such temperatures over time, untreated Teflon can warp; thus, it is recommended that Teflon slabs used in manufacturing an oven be pre-treated with heat prior to cutting/milling.

The OP-Cells (e.g., **Figs. S7e-f**) used in this polarizer have been described in the Main Document, but a few more details are provided here. First, given the safety issues involved, it is strongly encouraged that *any* OP-cell (be it ordered from the recommended supplier, or custom-

manufactured by another glassblower) be pressure-tested prior to use. All cells used in XeNA are pressure-tested on a vacuum/gas manifold up to ~45-50 psi (gauge pressure, above atmosphere) three times prior to use (i.e., prior to the first cleaning/loading steps). Next, an important feature of the cell design we use is that considerable additional effort must be expended (by the glassblower) to strengthen the weld between each window and the walls of the main 2" cylinder with a heavy internal fillet (**Fig. S7(f)**); such an effort may leave each window slightly curved/warped (which does not appear to negatively affect the SEOP performance). Finally, different OP-cell variants have different ways that they mate to the gas manifold of the polarizer. While the original variant shown in most of the pictures (e.g. **Fig. S7(e)**) terminates in ¼" Pyrex tubing that is attached to the manifold via ¼" PFA Swagelok fittings, this approach (while functional) is not particularly convenient for switching out cells. Two other approaches we have used include: (i) the addition of a glass adapter piece that uses an easy-to-remove Chem-Thread (o-ring) seal that adapts to the cell's ¼" Pyrex tubing (and is itself PFA-Swagelok connected to flexible tubing); and (ii) a design where the cell terminates in a smaller ChemThread fitting that can accommodate 1/8" flexible PTFE tubing from the polarizer's manifold.

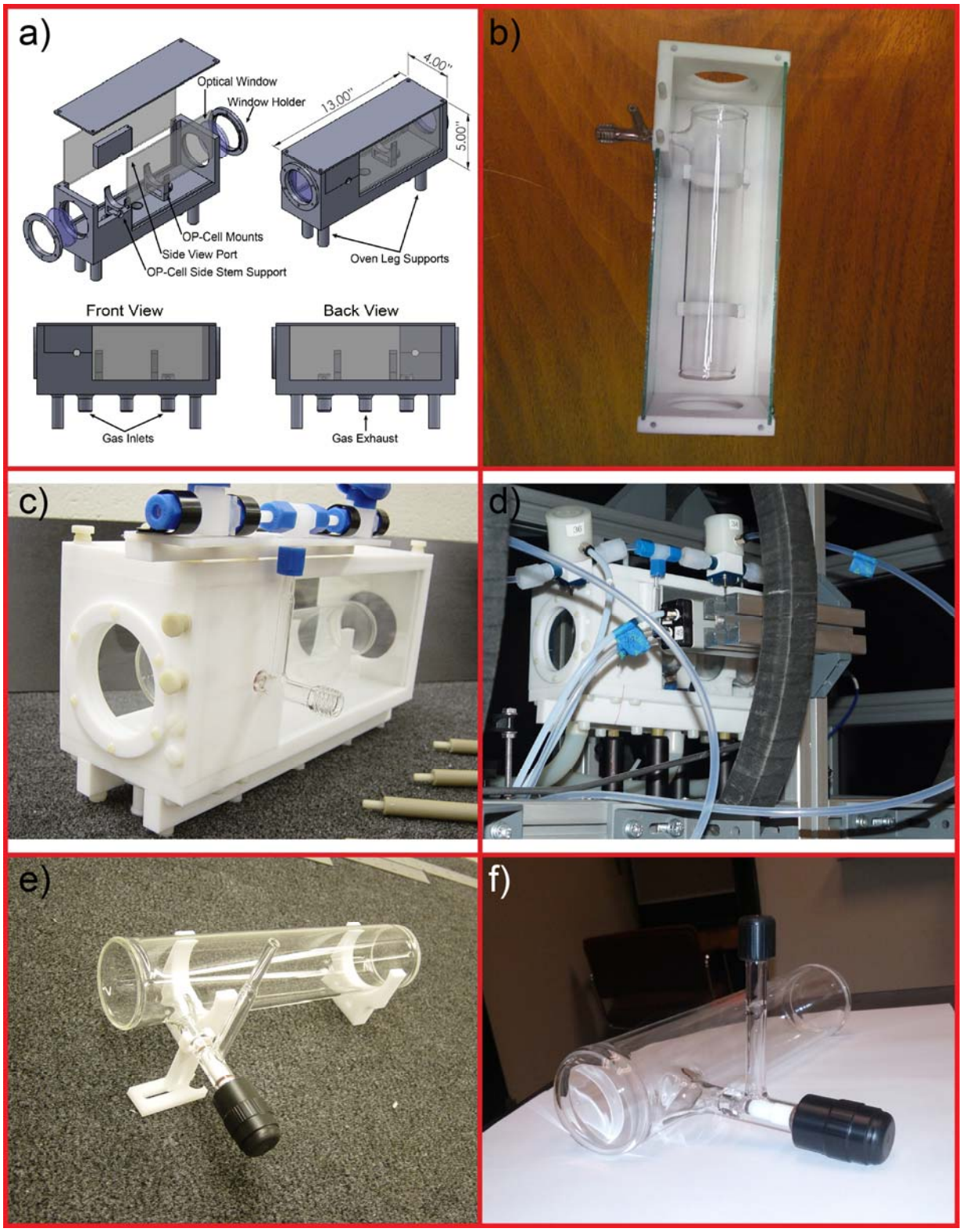

Figure S7. (a) CAD drawings showing different views of the optical pumping oven machined from Teflon sheets to accommodate the optical pumping cell. (b) Top view of machined Oven with OP-cell placement; *disclosure*: this photo has been altered to remove extraneous items from view. (c) Angled view of Oven at early stages of polarizer completion, well prior to automation. (d) Oven with automated valves installed in XeNA during a developmental stage; the Garolite posts supporting the oven are in view, as well as the silicone tubing delivering heated/cooled gases for temperature-management). The mounting plate for valve 36 is not in place. (e) An early design for an OP-cell, shown with the mounting pieces for the cell (made from Teflon). (f) Recently designed OP-Cell, exhibiting curved windows and a Chem Thread-terminated mounting port.

f) Graphical User Interface: As described below, all source codes for the software used to run the polarizer have been made freely available. The GUI was designed and programmed in software obtained from Processing.org, and provides a visual interface for the user to link the automation code of the Arduino microcontroller with "clickable" button functionality on the computer's display. The Arduino code and GUI can be modified to suit the user's needs. As shown in **Fig. S8**, the polarizer can be operated in either manual or automated mode.

The automation mode itself can operate in a number of different capacities, depending on what the user's needs are. The layout of the entire "Gas Manifold" is displayed in the upper portion of the GUI. The valves of the gas manifold (represented by the letter "V" followed by the valve number) can be manually operated by simply clicking on them. Under the "Utility" section, there are automated procedures for installing fresh gas cylinders, in which the messaging display will prompt the user to follow instructions to safely and properly install new cylinders.

Under the "Loading" section there are buttons for loading the ^{129}Xe gas, separated into two sections: pressures equal to or below 800 Torr, and pressures above 1200 Torr. This two-part separation was implemented because of the nature of the polarizer's gas pressure sensing. Pressures beyond 800 Torr may result in sensor failure of the Teledyne gauge used to measure vacuum. On the other hand, the Omega ('coarse') gauge is less accurate at reading low pressures, and is relied upon for for ensuring proper filling of the cell to ~2000 Torr total pressure. As a result, if loading ^{129}Xe densities below 800 Torr, the automated sequence is programmed to load ^{129}Xe gas first into the OP-cell. However, if loading ^{129}Xe densities above 1200 Torr, N_2 gas is loaded first (up to ~800 Torr) and back-filled to 2000 Torr total with ^{129}Xe gas. There are also options for loading the OP-cell with pre-mixed ^{129}Xe/N_2 gas cylinders. The button labeled "Set Stored Xe Pressure" is used to store in ^{129}Xe/N_2.

[continued…]

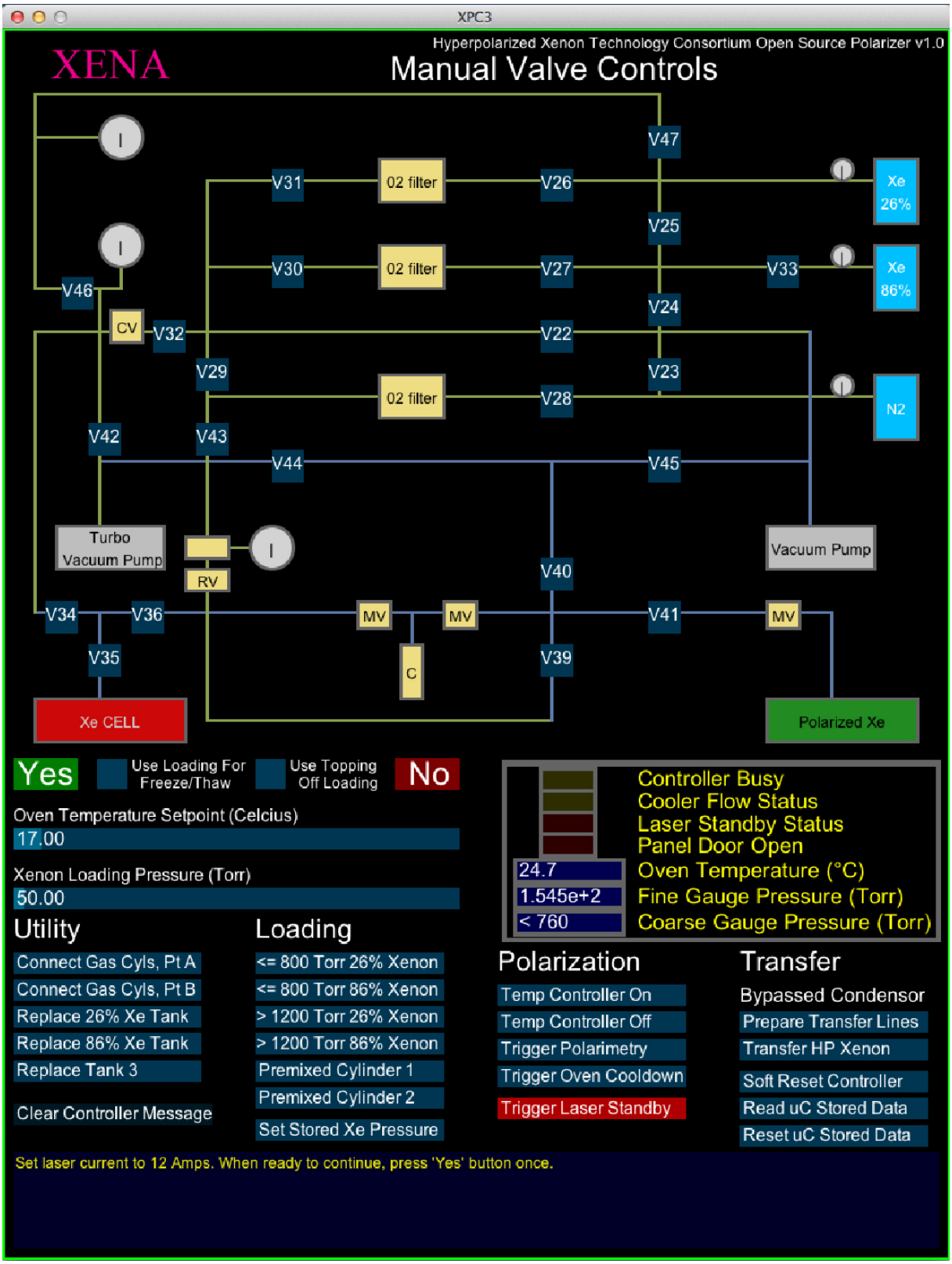

Figure S8. Graphical User Interface used to operate XeNA. Standard operation utilizes automation mode, whereas manual mode is for use by advanced users.

gas density loaded to the Arduino memory for the purpose of loading the OP-cell using the "Topping Off" procedure. After HP ^{129}Xe gas in transferred out of the OP-cell (e.g., to inflate a Tedlar bag), the pressure equilibrates leaving a good fraction of HP ^{129}Xe behind at ambient (~1 atm) pressure. If the user opts to use enriched (expensive) ^{129}Xe; rather than waste it by evacuating the cell in preparation for the next load, it can be saved to contribute to the cell loading for the next run. The way the automated loading procedures accomplishes this is by measuring the in-cell pressure of the remaining fraction, and using the original loading pressures stored in the Arduino to calculate the partial pressures of ^{129}Xe and N_2 gas that need to be reloaded into the cell to achieve the final desired in cell ^{129}Xe/N_2 gas density. This "topping off" procedure also helps to increase the duty cycle of the polarizer.

The GUI also has displays that let the user know the status of the microcontroller, water-flow sensor, and laser, in addition to displaying the oven temperature and fine and course pressure gauge pressures. The desired ^{129}Xe loading pressure and oven temperature can be set by using the sliding bars located above the "Utility and Loading" buttons. Moreover, the temperature control can be turned on and off, and the Kea2 low-field NMR spectrometer can be triggered via the GUI. If the user desires to cryo-collect the HP ^{129}Xe gas, there is a button in the GUI that when selected will change the automated transfer procedure used. Most buttons on the GUI are self-explanatory, which greatly simplifies operating this otherwise rather-complex device.

The Arduino and Processing source codes are freely available online for download from a Dropbox shared link at the following web address: https://www.dropbox.com/sh/g0gskqcobrm49yd/jMtrFKzTgu. The source codes will be maintained and be made available through this link for as long as possible. In the event that the link fails, please feel free to contact the corresponding authors for access to these files.

g) *In situ* monitoring of $\langle P_{Rb} \rangle$. The reader is directed to Refs. [S1,S2] for additional information, background, and examples concerning the content of this section. As shown in **Fig. S7**, the polarizer's oven contains window panels to allow not only visual inspection and alignment, but (in principle) also to allow one to probe the SEOP process via optical probe beam techniques (e.g., measuring the Rb electronic spin polarization via optically detected ESR), if one has the requisite additional instrumentation. Instead, for this work we have used a more indirect approach to estimate $\langle P_{Rb} \rangle$, the global average of the Rb polarization throughout the cell. The principle of this simple and quick approach is shown schematically in **Fig. S9a** [S1]. When the external magnetic field B_0 is 'off' (*left*), optical pumping is highly inefficient, and the ground electronic spin states will have nearly equal populations. Correspondingly, there will be a relatively high density of absorbers in the gas phase. However, when the magnetic field is turned 'on' along the quantization axis provided by the circularly polarized pump laser (*right*), optical pumping becomes much more efficient—resulting in highly unequal

populations of the ground magnetic sublevels, and hence increased transmission of the optical pumping laser through the cell.

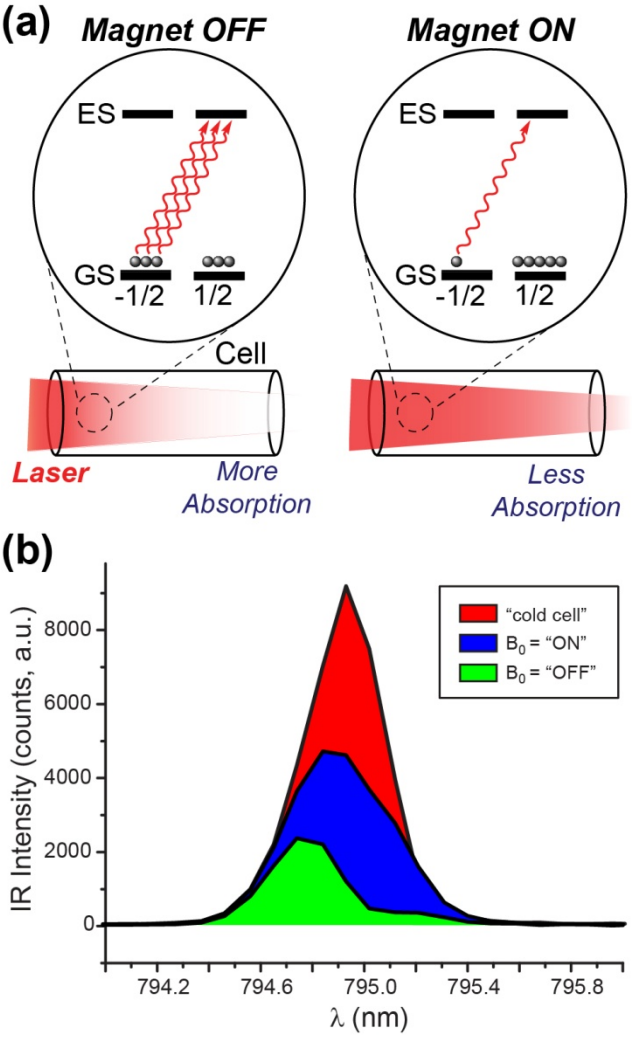

Figure S9. (*a*) Cartoon showing effects of magnetic field cycling on laser transmission in the context of depletion optical pumping of Rb electron spins [S1]; the drawings assume σ+ circularly polarized light, and Rb nuclear spin levels are not shown for simplicity.(*b*) Example of *in situ* monitoring of $\langle P_{Rb} \rangle$ using the near-IR spectra of pump laser transmission: at room temperature ("cold cell", red); 65°C and B_0=5.26 mT (blue); and 65 °C and B_0=0 mT (green).

During SEOP, the pump laser's spectral profile (as transmitted through the OP-cell) is monitored behind the retro-reflection mirror via a fiber optic probe (**Fig. S6**) that is connected to a high-resolution near-IR spectrometer (Ocean Optics HR2000+). Spectra are collected when the polarizer's electromagnet is alternately turned off and on, and compared to corresponding spectra obtained when the cell is cool (with a ventilated oven). The spectra can then be integrated and an estimate of the Rb polarization can be calculated using:

$$\left|\left\langle P_{Rb} \right\rangle\right| = \frac{A}{A_0} - 1,$$

where A and A_0 are respectively the cell absorbances for the (resonant) laser with and without the presence of the applied magnetic field from the polarizer's electromagnet (calculated, e.g. using A=-ln(I/I_0), where I and I_0 are the integrated intensities of the transmitted laser spectra with a 'hot' cell (e.g. during SEOP) and 'cold' cell, respectively [S2]). **Fig. S9b** shows examples for a cell containing 495 Torr Xe and 1300 Torr N_2 gas, corresponding to a value of $\langle P_{Rb} \rangle$~72%. Obtaining several acquisitions under each condition allows statistics for the measurement to be calculated, with most of the spectrum-to-spectrum variation owing to jitter from the laser (and the spectrometer) and actual changes in laser transmission from conditions within the cell (particularly if turbulent conditions are present). Additionally, as pointed out in Refs. [S1, S2], the method is potentially susceptible to two systematic errors: (1) measurement along the cell's center will tend to give a number that overestimates $\langle P_{Rb} \rangle$ (as the illumination will generally be poorer near the out regions of the cell); and (2) residual magnetic fields oriented along the direction of the pump laser (when the polarizer's electromagnet is off) will tend to allow Rb optical pumping with non-zero efficiency—causing an underestimate of $\langle P_{Rb} \rangle$. The former issue can be mitigated by taking measurements from other

positions, whereas the latter issue can be mitigated by orienting the polarizer perpendicular to any residual (e.g. Earth's) field, or by applying a field perpendicular field to the laser during the "magnet off" acquisitions.

h) ^{129}Xe Polarization Calibration: Examples of *in situ* low-field ^{129}Xe NMR are shown in Fig. 5 of the Main Document. Calibration of the ^{129}Xe nuclear spin polarization is performed by comparison with corresponding ^{1}H NMR spectra obtained at the same Larmor frequency using an identical cell filled with water doped with 5 mM copper sulfate, signal-averaged over an extended period of time (e.g., **Fig. S10a,b**) [S1]. The noise statistics from the FID are used to determine the error for the integral of the ^{1}H NMR signal (here, ~5.7% relative error), which is the dominant source of uncertainty for the P_{Xe} calculations. The in-cell P_{Xe} value can then be calculated for a given run in a straightforward manner from the ratio of the ^{129}Xe and ^{1}H NMR spectral integrals, taking into account: the ^{129}Xe and ^{1}H spin densities; the thermal nuclear spin polarization at (here) 62 kHz; and the effective tip angles of the RF pulses (ideally chosen to be the same by setting the RF powers the same, with relative pulse widths to be equal to the gyromagnetic ratios).

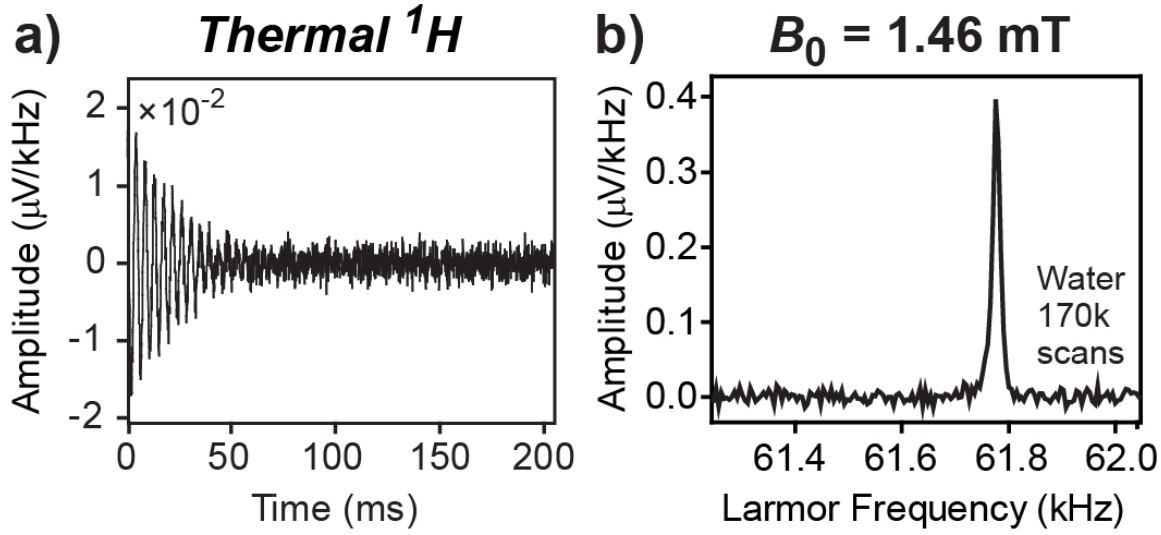

Figure S10. (a) ^{1}H Free induction domain (FID) spectrum from an OP-cell filled with water, 111 M ^{1}H concentration, doped with 5 mM copper sulfate, thermally polarized at 1.46 mT (62.0 kHz Larmor frequency; 170,000 scans; $\tau_{30°}$=16 μs; TR=0.3 s; P_H=5.0×10^{-9}); (b) Corresponding frequency domain NMR spectrum after Fourier transformation [S1].

i) OP-Cell Cool-down procedure: Because XeNA operates in batch/stopped-flow modes, the OP-cell generally must be cooled below operational SEOP temperatures prior to Xe transfer from the cell to a given sample, container, or transport vessel (e.g. Tedlar bag), in order to allow the Rb vapor to re-condense along the cell walls. However, this step is somewhat non-trivial because the laser itself is a significant source of heat for the cell (in addition to the oven heaters). In early efforts, we attempted

rapid cell cool-down by turning off oven heaters and the laser, while flash-cooling the cell with cool N_2 gas from the self-pressurized dewar, or, by performing this procedure while the laser driver current is ramped down as the cell is cooled. Both procedures allow the cell to be cooled in just 2-3 minutes, but the corresponding losses suffered during those few minutes because of high densities of "dark" Rb were too large (generally several fold; note that simply turning the driver current down will also result in the laser being (de)tuned from resonance). To mitigate such loses, we instituted a OP-cell cool-down procedure, a.k.a. 'Nikolaou on-resonance cool down', whereby we would rapidly cool-down the OP-cell while decreasing the resonant laser power to reduce the heat load, *while also* remaining on the Rb D_1 resonance—thus providing sufficient illumination for the declining [Rb] to largely avoid the "dark Rb" problem. As shown in Fig. S4, reducing the LDA driving current while maintaining the output centroid wavelength requires simultaneous adjustment of the LDA temperature (and hence, chiller temperature). Rather than tediously entering set temperatures from a table over time, instead we have instituted the following simple procedure: When the oven heaters are turned off, the LDA's water chiller is set to a higher temperature—e.g., one where the LDA would be on resonance at a low driving current just above the lasing threshold. Then, one (manually) slowly ramps down the LDA driving current over tens of seconds—at a rate that keeps the laser position fixed on resonance, countering the tendency of the laser to red-shift from position at the higher chiller temperature—using the transmitted laser spectrum as feedback. This process may be followed until the target HP ^{129}Xe gas transfer OP-cell temperature (e.g. 40 °C) is achieved. This cell-cooling process generally requires <5 min, a little longer than a simple rapid cool down with N_2 gas, but provides much higher P_{Xe} at the time of transfer. Data from our first implementation of this procedure is shown in **Fig. S11**, where "only" a ~26% loss in P_{Xe} is suffered by the time the OP-cell reaches the transfer temperature. However, later optimization of this procedure (with practice) results in much more modest losses, generally as little as a few percent. Furthermore, we note that this procedure (particularly with a different PSU for the LDA) could be pre-programmed into the polarizer, or automated with near-IR spectrometer feedback—increasing the polarizer's ease of operation.

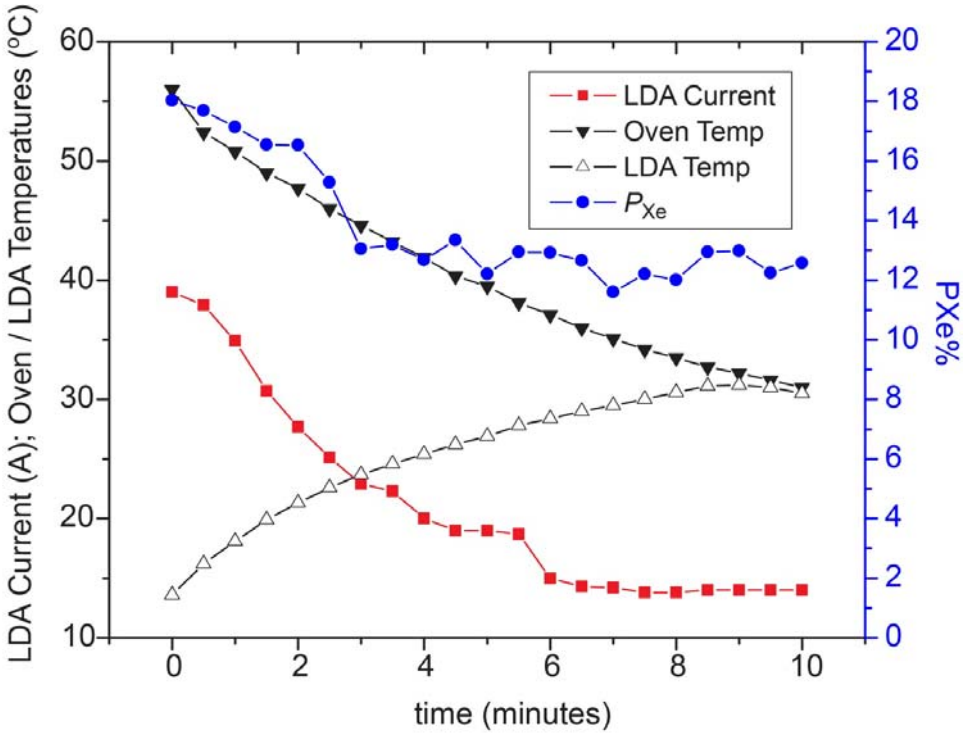

Figure S10. Graph showing the relatively small decay in P_{Xe} suffered during our first attempt at performing the OP-cell cool-down procedure described in the text. The graph also shows the simultaneous changes in LDA driving current, oven cell temperature, and LDA (chiller) temperature. An oven temperature of ~40 ºC is appropriate for HP ^{129}Xe transfer, according to our analysis of the contents of Tedlar bags under our conditions [S1].

j) Tedlar Bags and HP ^{129}Xe Transfer Procedure: Tedlar bags (e.g. 1 L) with a single polypropylene valve fitting (**Fig. S11a**) are modified and used to transfer HP ^{129}Xe from the OP-cell (SKC Inc., P/N 231-01). The polypropylene fitting is modified by first removing the top knob cap used to open and close the valve fitting. Once removed a ¼ in. O.D. septum is exposed that is used for mounting a ¼" Swagelok PFA manual valve (**Fig. S11b** - Swagelok, P/N PFA-43S4). However, before modification can be accomplished one more step must be taken. The horizontal extruding side septum (1/8 in. O.D.) is a part of the threaded nut used to compress the Tedlar bag between itself and the base of the valve fitting locating inside the Tedlar bag to create a tight seal. Unfortunately, this nut is tall and obstructs the Swagelok PFA valve from being attached to the ¼ in. exposed septum. To solve this problem, the threaded nut is removed and then cut in (more than) half, beginning immediately below the horizontal extruding stem, and then re-attached to the Tedlar bag. Once the Swagelok PFA valve is attached, the Tedlar bag can be connected to the downstream section of the gas manifold to pneumatic valve 41 (**Fig. S8**) via ¼ in. Teflon tubing.

Once the Tedlar bag is attached, the manual PFA valve is set to the open position, and the GUI command button labeled "Prepare Transfer Lines" is used to perform N_2 purge cycles. This procedure is performed while HP ^{129}Xe gas is being prepared in the OP-cell, and works by inflating the Tedlar bag

with N_2 and and evacuating with “rough” vacuum three times each. The N_2 gas is loaded into the Tedlar bag by allowing the gas to flow for a pre-set amount of time at 45 psi (gas tank regulator outlet pressure). Once complete the vacuum to the Tedlar back is switched from the rough pump to the Turbo pump to achieve high vacuum until HP ^{129}Xe is ready for transfer—thus leaving valve 40 and 41 open at the end of this procedure. If the transfer of HP ^{129}Xe is aborted, then the microcontroller must be reset to put all automated valves back to their natural state. Once the SEOP process is complete and the OP-cell is cooled, the HP ^{129}Xe gas can be transferred by using the GUI command button labeled “Transfer HP Xenon”. The first step in this sequence is to close pneumatic valve 40, thus shutting off vacuum in the transfer lines. This is immediately followed by opening valves 35 and 36 to allow the flow of HP ^{129}Xe gas to the Tedlar bag, which inflates in ~5 seconds before all actuated valves are closed. Once the Tedlar bag is inflated, the user must then manually close the Swagelok PFA to seal the HP gas inside. The Swagelok PFA valve can then be detached from the ¼ in. Teflon tubing connected to valve 41 and used for MRS/MRI experiments.

.

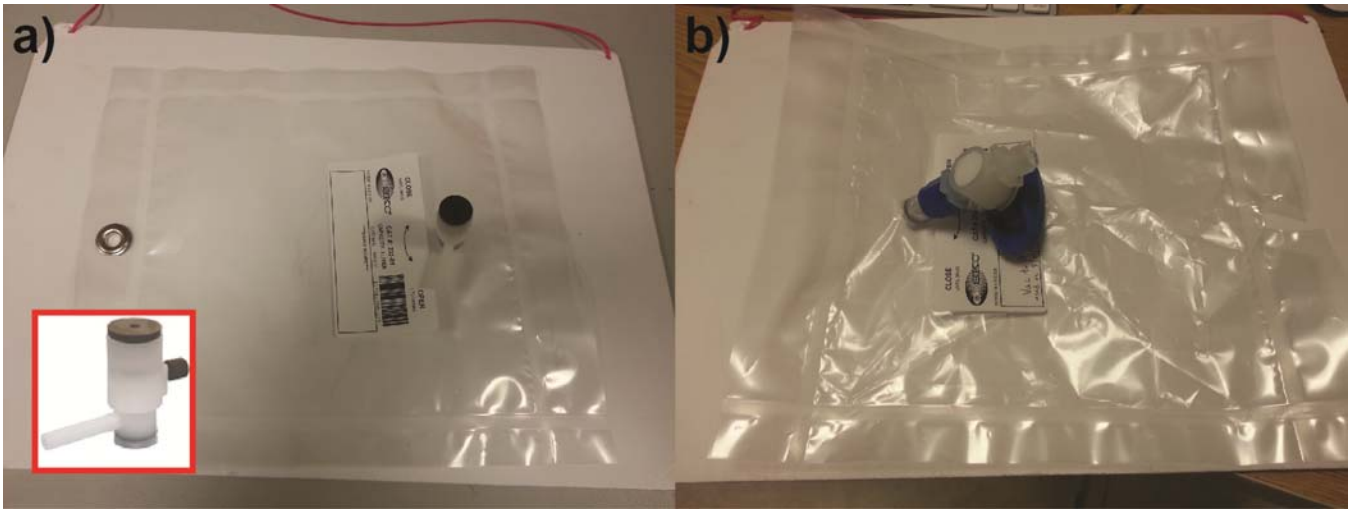

Figure S11. (a) Tedlar bag, as-is from the manufacturer. ***Inset:*** Polypropylene valve fitting delivered with this particular Tedlar bag. (b) Modified Tedlar bag with Swagelok PFA valve installed, now ready for use with XeNA.

SI References

[S1] Nikolaou, P., Coffey, A., Walkup, L., Gust, B., Whiting, N., Newton, H., Barcus, S., Muradyan, I., Moroz, G.D., Rosen, M., Patz, S., Barlow, M.J., Chekmenev, E., and Goodson, B.M., *Near-unity nuclear polarization with an open-source ^{129}Xe hyperpolarizer for NMR and MRI.* Proc. Natl. Acad. Sci. USA, 2013. **110**(35): p. 14150–14155.

[S2] Nikolaou, P., Whiting, N., Eschmann, N.A., Chaffee, K.E., Goodson, B.M., and Barlow, M., *Generation of Laser-Polarized Xenon Using Fiber-Coupled Laser Diode Arrays Narrowed with Integrated Volume Holographic Gratings.* J. Magn. Reson, 2009. **197**(2): p. 249-254.